Pergamon

PII: S0892-9270(96)00012-7

Space Technol. Vol. 16, No. 3, pp. 153–160, 1996

0892-9270/96 $15.00 + 0.00

A NEW SOFTWARE TOOL FOR LIMB SOUNDER MEASUREMENT SCENARIO SIMULATION*

G. ALBERTI,[1] M. GRASSI[2]† and S. MATTEI[1]

[1]Consortium for Research on Advanced Remote Sensing Systems (CO.RI.S.T.A.), Piazzale Tecchio 80, 80125, Naples, Italy and [2]Dip. Scienza e Ingegneria dello Spazio "L.G. Napolitano", University of Naples "Federico II", Piazzale Tecchio 80, 80125, Naples, Italy

Abstract—Observations of the troposphere in the millimeter wave region are of particular interest since some very important atmospheric trace gases are only accessible in this part of the electromagnetic spectrum. In the framework of European Space Agency (ESA) space programs for atmosphere chemistry analysis, a pre-phase "A" study of a new limb-sounder, MASTER (millimeter-wave acquisition for stratosphere/troposphere exchange research), has already started. One important task of this study is related to the development of a modular simulation program which generates antenna temperature maps, including Sun, Moon, Earth, atmosphere and cold space contributions, in order to define the future operative parameters of MASTER. This paper is aimed at describing the software tool and some simulation results. Copyright © 1996 Elsevier Science Ltd

INTRODUCTION

A full understanding of the atmosphere chemistry is of fundamental importance to predict changes in the Earth's climate and the composition of its atmosphere. A powerful tool is represented by the limb-sounding technique using passive microwave sensors, which offers several advantages for the study of the upper atmosphere [1] and for monitoring the concentration profiles of certain atmospheric species. Observations of the troposphere in the millimeter wave region are of particular interest since some very important atmospheric trace gases are only accessible in this part of the electromagnetic spectrum.

In this framework, the European Space Agency (ESA) is presently paving the way for microwave limb sounding missions, to be embarked on a satellite after the year 2000. One of the missions under consideration is MASTER (millimeter-wave acquisition for stratosphere/troposphere exchange research), whose pre-phase "A" study has already started.

MASTER instrument is to be a combined radiometer and spectrometer, with high spatial, radiometric and spectroscopic resolution, which performs passive monitoring of the atmosphere at the following main bands: (A) 199–207 GHz; (B) 296–306 GHz; (C) 318–326 GHz; (D) 342–348 GHz. The instrument is able to provide in the above bands 640 channels with a spectral sampling interval better than 50 MHz. In addition, two high spectral resolution channels (HSRC) are always available: one is fixed at 298.4 GHz and the other is moveable to any spectral region within the main bands. Both have a spectral sampling interval of 3 MHz over a width of 600 MHz, that means a total number of 400 high resolution channels. MASTER will fly on a spacecraft in a near circular orbit, sun-synchronous mission, looking to the rear of the spacecraft at the Earth's limb in the plane of the orbit [2].

A task of this study is related to the definition and implementation of a simulation program for MASTER instrument. The objective of the simulator is to generate temperature maps which include Sun, Moon, Earth, atmosphere and cold space contributions, in order to define the operative parameters of MASTER. The celestial objects are considered as extended blackbody sources, while for the atmosphere a built-in model is used. The software, implemented under MATLAB as a mathematical package, adopts graphic interfaces. The entire tool is composed of two parts:

- The simulation program: it generates the temperature maps and puts them into output files. To run it properly, four input files are required. The first must contain the orbital parameters; the second the atmosphere brightness temperature profile; the last two files contain the antenna directivity data. The users can define their own input files or use the default ones.
- The output program: it is a utility that helps the user to see the simulation results quickly by means of output windows. Two kinds of graphs can be plotted: one shows antenna temperature vs tangent height, for a given orbital position; the other gives antenna

*This work has been conducted under funding from the Earth Observation Programme of the European Space Agency.
†Corresponding author.

temperature vs orbital position, for a given tangent height. In both cases, the corresponding scenario is also displayed.

SIMULATION MODEL

The simulation program has been built following a modular architecture (Fig. 1). It is composed of two main modules: the scan/orbit module and the integration module.

Scan/orbit module

This module performs the evaluation of the radiation sources positions in the antenna-fixed reference frame. To this end, the following reference frames are introduced:

- The Earth-fixed inertial reference frame (X,Y,Z), whose origin is at the Earth's center, the X–Y plane coincides with the Earth's equatorial plane, the X-axis is directed toward the first point of Aries, and the Z-axis is directed toward the North Pole.
- The orbiting reference frame (x,y,z), whose origin is at the satellite center of mass, the z-axis is aligned with the satellite position vector $(\boldsymbol{R}_s)$ and directed toward the Earth, the x-axis is directed along the orbital velocity vector, and the y-axis completes a right-handed reference frame.
- The body reference frame (123), whose axes coincide with the satellite's principal of inertia axes.
- The boresight antenna reference frame (x_a,y_a,z_a), whose origin is at the antenna geometric center, the x_a–y_a plane coincides with the antenna plane, and the z_a-axis is directed toward the antenna boresight.

Figures 2 and 3 illustrate the above reference frames. The satellite attitude dynamics is simulated considering the yaw (γ), pitch (β) and roll (α) attitude angles as the Euler's angles of the satellite principal of inertia axes with respect to the orbiting reference frame (Fig. 2). The simulation also includes the satellite yaw steering maneuver [3]. The scan motion of the instrument antenna is simulated considering the azimuth (AZ) and elevation (E) angles of the antenna-fixed reference frame with respect to the satellite one (Fig. 3).

The evaluation of the radiation sources positions in the antenna-fixed reference frame is performed using a set of orthogonal matrices:

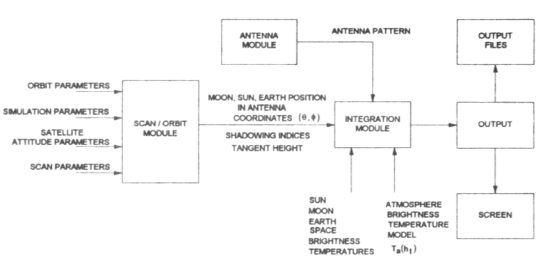

Fig. 1. Simulation program architecture.

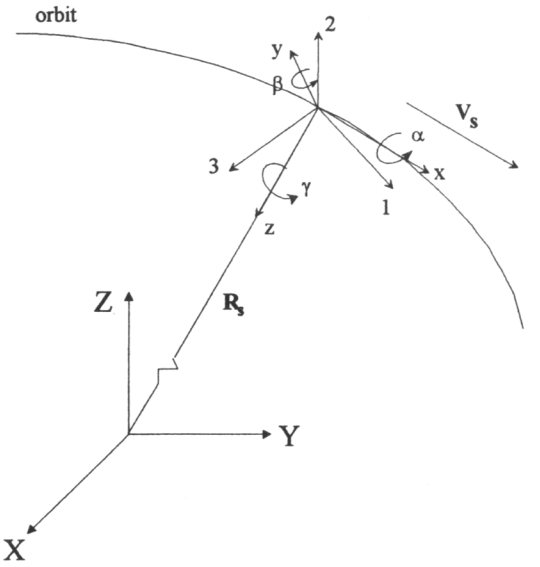

Fig. 2. Inertial, orbiting satellite-fixed reference frames.

M_{orb}, which performs the transformation from the inertial to the orbiting reference frame;

M_{ypr}, which performs the transformation from the orbiting to the satellite-fixed reference frame;

M_{scan}, which performs the transformation from the satellite to the antenna-fixed reference frame.

Then, the radiation source coordinates in the instrument antenna reference frame are evaluated as follows:

$$\begin{bmatrix} \boldsymbol{R}_{so_{xa}} \\ \boldsymbol{R}_{so_{ya}} \\ \boldsymbol{R}_{so_{za}} \end{bmatrix} = M_{\text{scan}} M_{\text{ypr}} M_{\text{orb}} \begin{bmatrix} \boldsymbol{R}_{so_x} \\ \boldsymbol{R}_{so_y} \\ \boldsymbol{R}_{so_z} \end{bmatrix} \tag{1}$$

where $\boldsymbol{R}_{so}$ is the radiation source power position vector (Fig. 3), and M_{scan}, M_{ypr} and M_{orb} are given by the following expressions [4]:

$$M_{\text{scan}} = \begin{bmatrix} \cos E \cos AZ & \sin AZ & -\cos AZ \sin E \\ -\cos E \sin AZ & \cos AZ & \sin E \sin AZ \\ \sin E & 0 & \cos E \end{bmatrix} \tag{2}$$

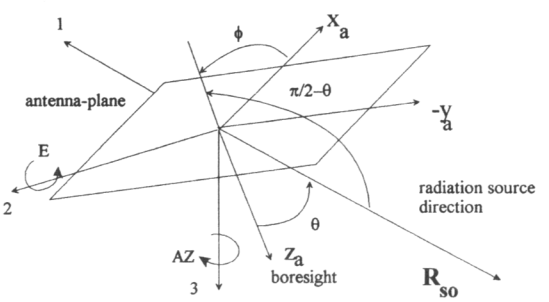

Fig. 3. Body and antenna-fixed reference frames.

$$M_{ypr} = \begin{bmatrix} \cos\beta\cos\gamma & \cos\beta\sin\gamma & -\sin\beta \\ -\cos\alpha\sin\gamma + \sin\alpha\sin\beta\cos\gamma & \cos\alpha\cos\gamma + \sin\alpha\sin\beta\sin\gamma & \sin\alpha\cos\beta \\ \sin\alpha\sin\gamma + \cos\alpha\sin\beta\cos\gamma & -\sin\alpha\cos\gamma + \cos\alpha\sin\beta\sin\gamma & \cos\alpha\cos\beta \end{bmatrix} \tag{3}$$

$$M_{orb} = \begin{bmatrix} \dfrac{[(-R_s \times V_s) \times (-R_s)]_x}{|(-R_s \times V_s) \times (-R_s)|} & \dfrac{[(-R_s \times V_s) \times (-R_s)]_y}{|(-R_s \times V_s) \times (-R_s)|} & \dfrac{[(-R_s \times V_s) \times (-R_s)]_z}{|(-R_s \times V_s) \times (-R_s)|} \\ \dfrac{(-R_s \times V_s)_x}{|R_s \times V_s)} & \dfrac{(-R_s \times V_s)_y}{|R_s \times V_s|} & \dfrac{(-R_s \times V_s)_z}{|R_s \times V_s|} \\ \dfrac{R_{s_x}}{|R_s|} & \dfrac{R_{s_y}}{|R_s|} & \dfrac{R_{s_z}}{|R_s|} \end{bmatrix} \tag{4}$$

where $\boldsymbol{R}_s$ and $\boldsymbol{V}_s$ are the satellite inertial position and velocity vectors. The positions of the radiation sources in the antenna-fixed reference frame are, finally, expressed in terms of the elevation (θ) and azimuth (ϕ) angles, defined as in Fig. 3.

Integration module

For a limb sounder the antenna radiometric temperature can be written as [5]

$$T_A = \frac{1}{4\pi}\iint_{4\pi} T_B(\theta,\varphi)D(\theta,\varphi)\,\mathrm{d}\Omega \tag{5}$$

where

$$\mathrm{d}\Omega = \sin\theta\,\mathrm{d}\theta\,\mathrm{d}\varphi\,, \tag{6}$$

θ, φ are the antenna coordinates, $T_B(\theta, \varphi)$ represents the equivalent radiometric temperature of the scene and $D(\theta, \varphi)$ is the antenna directivity.

For a radiometric measurement, the scene is decomposed into two distinct areas: the Main Beam (MB) region, over which the measurement is to be carried out, and the Side Lobe (SL) region, which takes into account contributions received from directions outside the Main Beam. Therefore, equation (5) can be written as

$$T_A = \frac{1}{4\pi}\iint_{MB} T_B(\theta,\varphi)D(\theta,\varphi)\,\mathrm{d}\Omega + \frac{1}{4\pi}\iint_{SL} T_B(\theta,\varphi)D(\theta,\varphi)\,\mathrm{d}\Omega\,. \tag{7}$$

The Main Beam and the Side Lobe regions are characteristic parameters of the given antenna directivity.

If the brightness temperature is constant over the scene, the antenna temperature becomes:

$$T_A = T_B\eta_{MB} + T_{ext} \tag{8}$$

where

$$T_{ext} = \frac{1}{4\pi}\iint_{SL} T_B(\theta,\varphi)D(\theta,\varphi)\,\mathrm{d}\Omega \tag{9}$$

is the external temperature that accounts for external contributions not coming from the scene which is being observed and

$$\eta_{MB} = \frac{1}{4\pi}\iint_{MB} D(\theta,\varphi)\,\mathrm{d}\Omega \tag{10}$$

is the *main-beam efficiency*.

Antenna module. The simulation program uses 2-D antenna directivity function which is generated by interpolating input data containing the antenna directivity sampled in the u–v plane. The user must provide u_{min}, u_{max}, v_{min}, v_{max} and u_3, v_3 parameters values delimiting the sampling region and the Main Beam region of the antenna directivity, respectively. The module then calculates the Main Beam region as

$$\begin{aligned} \theta_3 &= \sin^{-1}(u_3) \\ \varphi_3 &= \sin^{-1}(v_3) \\ MB(u) &= \frac{5}{4}\theta_3 \\ MB(v) &= \frac{5}{4}\varphi_3 \end{aligned} \tag{11}$$

and the Side Lobe region as everywhere in the sampling region but the Main Beam region. The beam efficiency is also computed as follows:

$$\eta = \eta_\delta\eta_s\eta_{MB} \tag{12}$$

where η_δ accounts for scattering losses and η_s accounts for spill-over losses. In our model, we make the assumption that η_δ and η_s are equal to 1.

Radiation sources characterization. The total brightness measured by the instrument is considered as the sum of the contributions coming from different radiation sources. In our model, the contributions from Earth, atmosphere, Moon, Sun and cold space are taken into account: Earth, Moon and Sun are modeled as blackbody extended spherical sources, cold space is modeled as blackbody extended source, while the Earth's atmosphere is considered as an emitting wall at horizon with emissivity independent of frequency. The antenna temperature is therefore given by

$$T_A = T_A^E + T_A^{At} + T_A^M + T_A^S + T_A^{CS} \tag{13}$$

where T_A^E, T_A^{At}, T_A^M, T_A^S, T_A^{CS} indicate the antenna temperature due to the Earth, atmosphere, Moon, Sun and cold space contributions, respectively. They are computed as described in the following.

Earth

In our assumption, the antenna temperature due to Earth's emission can be written as:

$$T_A^E = \frac{1}{4\pi} T_E \iint_{(\theta,\varphi)\in \text{Earth}} D(\theta,\varphi) \sin\theta \, d\theta \, d\varphi \quad (14)$$

where T_E is the brightness temperature of the Earth. The integral in (14) can be more easily calculated if instead of the (θ, φ) coordinates in the boresight antenna reference frame we use the (θ_d, φ_d) coordinates in a new reference frame rotated with respect to the former so that its z-axis is pointed towards the center of the Earth. In this case, φ ranges over $[0, 2\pi]$ and θ ranges over $[0, \Delta\theta_E]$, where $\Delta\theta_E$ represents the angular semi-aperture of the Earth.

Hence, we have:

$$T_A^E = \frac{1}{4\pi} T_E \int_0^{2\pi}\int_0^{\Delta\theta_E} D'(\theta_d,\varphi_d) \times \frac{1}{\sqrt{1-u^2-v^2}} J(\theta_d,\varphi_d) \, d\theta_d \, d\varphi_d \quad (15)$$

where $D'(\theta_d, \varphi_d)$ is the antenna directivity calculated at (θ_d, φ_d) position, $J(\theta_d, \varphi_d)$ is the jacobian of the transformation given by

$$J(\theta_d,\varphi_d) = (M_{11}M_{22} - M_{12}M_{21}) \sin\theta_d \cos\theta_d + (M_{12}M_{32} - M_{22}M_{31}) \sin^2\theta_d \cos\varphi_d \quad (16)$$

and

$$u = \sin\theta\cos\varphi = M_{11}\sin\theta_d\cos\varphi_d + M_{21}\sin\theta_d\sin\varphi_d + M_{31}\cos\theta_d$$

$$v = \sin\theta\sin\varphi = M_{12}\sin\theta_d\cos\varphi_d + M_{22}\sin\theta_d\sin\varphi_d + M_{32}\cos\theta_d$$

$$M(\theta_E,\varphi_E) = \begin{bmatrix} \cos\theta_E\cos\varphi_E & \cos\theta_E\sin\varphi_E & -\sin\theta_E \\ -\sin\varphi_E & \cos\varphi_E & 0 \\ \sin\theta_E\cos\varphi_E & \sin\theta_E\sin\varphi_E & \cos\theta_E \end{bmatrix} \quad (17)$$

The matrix M defines the transformation between the boresight and the rotated antenna reference frame. (θ_E, φ_E) represents the position of the center of the Earth in the boresight antenna reference frame. Since the Earth's brightness temperature is considered constant over the scene, using equation (7), equation (15) becomes

$$T_A^E = \frac{1}{4\pi} T_E \left(\iint_{MB} f(\theta_d,\varphi_d) \, d\theta_d \, d\varphi_d + \iint_{SL} f(\theta_d,\varphi_d) \, d\theta_d \, d\varphi_d \right) \quad (18)$$

where

$$f(\theta_d,\varphi_d) = D'(\theta_d\varphi_d) \frac{1}{\sqrt{1-u^2-v^2}} J(\theta_d,\varphi_d)$$

$$\iint_{SL} f(\theta_d,\varphi_d) \, d\theta_d \, d\varphi_d = (1-\eta)\Omega_{SL}^E . \quad (19)$$

In the above relations, Ω_{SL}^E represents the fraction of the Earth's solid angle that falls into the Side Lobe region.

Atmosphere

The antenna temperature due to the atmosphere contribution can be written as:

$$T_A^{At} = \frac{1}{4\pi} \int_0^{2\pi}\int_{\theta_{d\min}}^{\theta_{d\max}} T_{At}(h_t) D'(\theta_d\varphi_d) \times \frac{1}{\sqrt{1-u^2-v^2}} J(\theta_d,\varphi_d) \, d\theta_d \, d\varphi_d . \quad (20)$$

θ_d can be expressed as a function of the tangent height, h_t, as follows

$$\theta_d = \Delta\theta_E + tg^{-1}\left(\frac{h_t}{\sqrt{(R_E + H)^2 - R_E^2}} \right) \cong \Delta\theta_E + \frac{h_t}{\sqrt{(R_E+H)^2 - R_E^2}} \quad (21)$$

where H is the satellite altitude and R_E is the Earth's radius. The integration limits are then given by

$$\theta_{d_{\min}} = \Delta\theta_E \ (h_t = 0 \text{ km})$$

$$\theta_{d_{\max}} = 0.0304 \ (h_t = 100 \text{ km}; H = 800 \text{ km}) . \quad (22)$$

The brightness temperature of the atmosphere, $T_{At}(h_t)$, is a function of the tangent height, given by [1]

$$T_{At}(h_t) = T_{CS} e^{-\tau(h_t, z_{\max})} + \int_{h_t}^{z_{\max}} T(z) W_T(z) \, dz \quad (23)$$

where T_{CS} is the cold space brightness temperature and

$$W_T(z) = \bar{k}_{H_2O}(z) e^{-\tau(h_t,z_{\max})} (1 + e^{-2\tau(h_t,z_{\max})}) f(z)$$

$$\tau(z_1,z_2) = \int_{z_1}^{z_2} \bar{k}_{H_2O}(z) f(z) \, dz$$

$$f(z) = (R_E + z)[(R_E + z)^2 - (R_E + h_t)^2]^{-1/2} \quad (24)$$

In these equations z represents the atmospheric altitude in km, $z_{\max}$ is the maximum atmosphere altitude (90 km), h_t is the tangent height in km, R_E is the Earth's radius in km and $T(z)$ is the actual atmospheric temperature profile in Kelvin. Since, in our assumption, the emissivity of the atmosphere is independent of frequency, the coefficient $\bar{k}_{H_2O}(z)$ has been calculated, for each altitude, as the mean value of the water vapor absorption coefficient over 200–300 GHz frequency range. Only water vapor has

been taken into account since it is the most effective molecule that emits within the instrument operative spectral range. The water vapor absorption spectrum in dB/km used for the computation is given by [5]

$$k_{H_2O}(f) = k_{H_2O}'(f) + \Delta k(f) \tag{25}$$

where f is the frequency and

$$k_{H_2O}'(f) = 2f^2\rho_v\left(\frac{300}{T}\right)^{5/2}\sum_{i=1}^{10} A_i e^{-E_i/T}\left(\frac{\gamma_i}{(f_i^2 - f^2)^2 + 4f^2\gamma_i^2}\right)$$

$$\Delta k(f) = 4.69 \times 10^{-6}\rho_v\left(\frac{300}{T}\right)^{2.1}\left(\frac{P}{1000}\right)f^2. \tag{26}$$

In the above relations:

P is the atmospheric pressure profile in millibars given by

$$P(z) = P_0 e^{-z/H_3} \tag{27}$$

where P_0 is the sea-level pressure and H_3 is the pressure scale height;

ρ_v is the water vapor density profile in grams per cubic meter given by

$$\rho_v(z) = \rho_{v0} e^{-z/H_4} \tag{28}$$

where ρ_{v0} is the sea-level water vapor density and H_4 is the water vapor density scale height;

T is the atmospheric temperature profile in Kelvin;

γ_i is the linewidth parameter in GHz given by

$$\gamma_i = \gamma_{i0}\left(\frac{P}{1013}\right)\left(\frac{300}{T}\right)^{x_i}\left[1 + 10^{-2}a_i\frac{\rho_v T}{P}\right]. \tag{29}$$

The values of the coefficients a_i, e_i, f_i, γ_{i0}, a_i and x_i are given in [5].

Figure 4 shows the brightness atmosphere temperature $T_{At}(h_t)$ as a function of the tangent height,

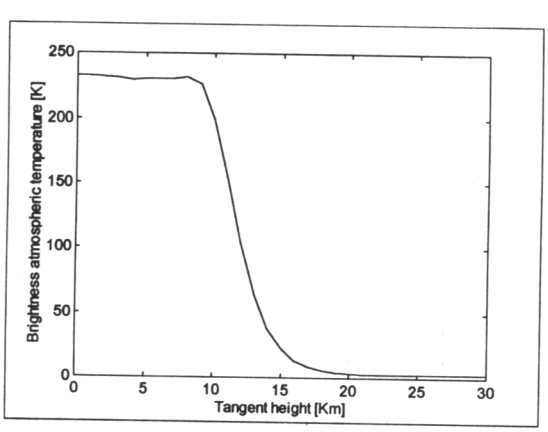

Fig. 4. Brightness atmospheric temperature vs tangent height.

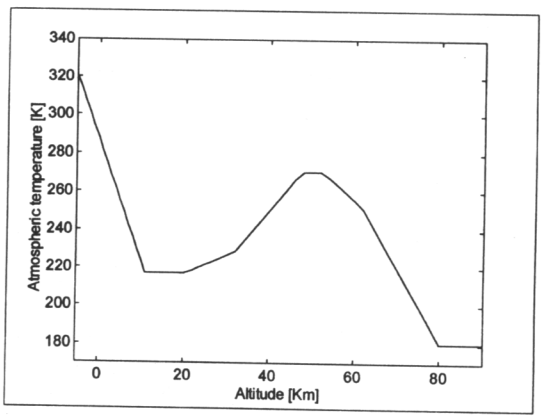

Fig. 5. Atmospheric temperature profile vs altitude.

computed using the temperature profile shown in Fig. 5 and the parameters listed below

Parameter	Symbol	Value
Altitude	z	0–90 km
Tangent height	h_t	0–30 km
Earth's radius	R_E	6378 km
Sea-level pressure	P_0	1013 mbar
Pressure scale height	H_3	7.7 km
Sea-level H_2O density	ρ_{v0}	7.72 g/m^3
H_2O density scale height	H_4	2 km

Using equation (7), equation (20) becomes

$$T_A^{At} = \frac{1}{4\pi}\left(\iint_{MB} f(\theta_d,\varphi_d)\,d\theta_d\,d\varphi_d + \iint_{SL} f(\theta_d,\varphi_d)\,d\theta_d\,d\varphi_d\right) \tag{30}$$

where

$$f(\theta_d,\varphi_d) = T_{At}'(\theta_d)D'(\theta_d\varphi_d)\frac{1}{\sqrt{1-u^2-v^2}}J(\theta_d,\varphi_d) \tag{31}$$

Moon

Let us indicate T_M as the brightness temperature of the Moon. The antenna temperature due to the Moon's contribution can be written as

$$T_A^M = F_M\left[\frac{1}{4\pi}T_M\int_0^{2\pi}\int_0^{\Delta\theta_M} D''(\theta_d'\varphi_d') \times \frac{1}{\sqrt{1-u^2-v^2}}J(\theta_d',\varphi_d')\,d\theta_d'\,d\varphi_d'\right] \tag{32}$$

where

$$J(\theta_d',\varphi_d') = (M_{11}^M M_{22}^M - M_{12}^M M_{21}^M)\sin\theta_d'\cos\theta_d' + (M_{12}^M M_{32}^M - M_{22}^M M_{31}^M)\sin^2\theta_d'\cos\varphi_d'$$

$$u = \sin\theta\cos\varphi = M_{11}^M\sin\theta_d'\cos\varphi_d' + M_{21}^M\sin\theta_d'\sin\varphi_d' + M_{31}^M\cos\theta_d'$$

$$v = \sin\theta\sin\varphi = M_{12}^M\sin\theta_d'\cos\varphi_d' + M_{22}^M\sin\theta_d'\sin\varphi_d' + M_{32}^M\cos\theta_d'$$

$$M^M(\theta_M,\varphi_M) = \begin{bmatrix} \cos\theta_M\cos\varphi_M & \cos\theta_M\sin\varphi_M & -\sin\theta_M \\ -\sin\varphi_M & \cos\varphi_M & 0 \\ \sin\theta_M\cos\varphi_M & \sin\theta_M\sin\varphi_M & \cos\theta_M \end{bmatrix}. \quad (33)$$

(θ_M, φ_M) are the elevation and azimuth of the Moon's position vector in the boresight antenna reference frame, $\Delta\theta_M$ represents the angular aperture of the Moon, $D''(\theta'_d, \varphi'_d)$ is the antenna directivity calculated at (θ'_d, φ'_d) position and F_M is a coefficient that gives the percentage of the Moon's shadowing. F_M ranges from 0 to 1. Also in this case, using equation (7), equation (32) becomes:

$$T_A^M = \frac{1}{4\pi} T_M\left(\iint_{MB} f(\theta_d',\varphi_d')\,\mathrm{d}\theta_d'\,\mathrm{d}\varphi_d' + \iint_{SL} f(\theta_d',\varphi_d')\,\mathrm{d}\theta_d'\,\mathrm{d}\varphi_d'\right) \quad (34)$$

where

$$f(\theta_d',\varphi_d') = D''(\theta_d'\varphi_d')\frac{1}{\sqrt{1-u^2-v^2}} J(\theta_d',\varphi_d')$$

$$\iint_{SL} f(\theta_d',\varphi_d')\,\mathrm{d}\theta_d'\,\mathrm{d}\varphi_d' = (1-\eta)\Omega_{SL}^M \quad (35)$$

Ω_{SL}^M is the Moon's solid angle fraction that falls into the Side Lobe region.

Sun

If (θ_S, φ_S) is the elevation and azimuth of the Sun position vector in the boresight antenna reference frame and T_S is the Sun brightness temperature considered constant over the scene, the antenna temperature due to the Sun's contribution becomes

$$T_A^S = F_S\left[\frac{1}{4\pi} T_S\int_0^{2\pi}\int_0^{\Delta\theta_S} D'''(\theta_d''\varphi_d'') \times \frac{1}{\sqrt{1-u^2-v^2}} J(\theta_d'',\varphi_d'')\,\mathrm{d}\theta_d''\,\mathrm{d}\varphi_d''\right] \quad (36)$$

where

$$J(\theta_d'',\varphi_d'') = (M_{11}^S M_{22}^S - M_{12}^S M_{21}^S)\sin\theta_d''\cos\theta_d'' + (M_{12}^S M_{32}^S - M_{22}^S M_{31}^S)\sin^2\theta_d''\cos\varphi_d''$$

$$u = \sin\theta\cos\varphi = M_{11}^S\sin\theta_d''\cos\varphi_d'' + M_{21}^S\sin\theta_d''\sin\varphi_d'' + M_{31}^S\cos\theta_d''$$

$$v = \sin\theta\sin\varphi = M_{12}^S\sin\theta_d''\cos\varphi_d'' + M_{22}^S\sin\theta_d''\sin\varphi_d'' + M_{32}^S\cos\theta_d''$$

$$M^S(\theta_S,\varphi_S) = \begin{bmatrix} \cos\theta_S\cos\varphi_S & \cos\theta_S\sin\varphi_S & -\sin\theta_S \\ -\sin\varphi_S & \cos\varphi_S & 0 \\ \sin\theta_S\cos\varphi_S & \sin\theta_S\sin\varphi_S & \cos\theta_S \end{bmatrix} \quad (37)$$

$\Delta\theta_S$ represents the angular aperture of the Sun, $D'''(\theta_d'', \varphi_d'')$ is the antenna directivity calculated at $(\theta_d'', \varphi_d'')$ position and F_S is a coefficient, ranging from 0 to 1, that gives the percentage of the Sun shadowing. Using equation (7), equation (36) can be written as

$$T_A^S = \frac{1}{4\pi} T_S\left(\iint_{MB} f(\theta_d'',\varphi_d'')\,\mathrm{d}\theta_d''\,\mathrm{d}\varphi_d'' + \iint_{SL} f(\theta_d'',\varphi_d'')\,\mathrm{d}\theta_d''\,\mathrm{d}\varphi_d''\right) \quad (38)$$

where

$$f(\theta_d'',\varphi_d'') = D'''(\theta_d'',\varphi_d'')\frac{1}{\sqrt{1-u^2-v^2}} J(\theta_d'',\varphi_d'')$$

$$\iint_{SL} f(\theta_d'',\varphi_d'')\,\mathrm{d}\theta_d''\,\mathrm{d}\varphi_d'' = (1-\eta)\Omega_{SL}^S. \quad (39)$$

Ω_{SL}^S is the Sun's solid angle fraction that falls into the Side Lobe region.

Cold space

Because cold space is everywhere except the Sun, Moon, Earth and atmosphere, its contribution to the antenna temperature can be written as:

$$T_A^{CS} = \frac{1}{4\pi} T_{CS}\left[\iint_{4\pi} D(\theta,\varphi)\sin\theta\,\mathrm{d}\theta\,\mathrm{d}\varphi - \iint_{(\theta,\varphi)\in\text{Earth}} D(\theta,\varphi)\sin\theta\,\mathrm{d}\theta\,\mathrm{d}\varphi + - \iint_{(\theta,\varphi)\in\text{Atmosphere}} D(\theta,\varphi)\sin\theta\,\mathrm{d}\theta\,\mathrm{d}\varphi - \iint_{(\theta,\varphi)\in\text{Moon}} D(\theta,\varphi)\sin\theta\,\mathrm{d}\theta\,\mathrm{d}\varphi - \iint_{(\theta,\varphi)\in\text{Sun}} D(\theta,\varphi)\sin\theta\,\mathrm{d}\theta\,\mathrm{d}\varphi\right] \quad (40)$$

NUMERICAL SIMULATION

Several numerical simulations were performed to simulate different measurement scenarios and, therefore, to evaluate the antenna temperature contributions due to the different source emissions. In particular, in order to generate antenna temperature maps which include contributions from Sun, Moon, Earth, atmosphere and cold space four simulations were performed considering one orbit at autumn equinox, at winter solstice, at spring equinox and at summer solstice. The input parameters used in the various simulations are listed in the table below, while Figs 4 and 6 show the input brightness atmospheric

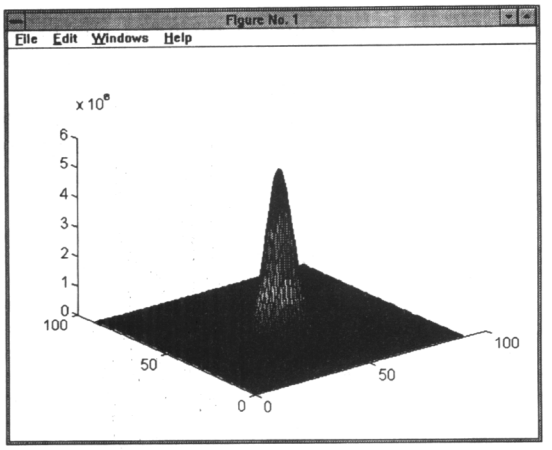

Fig. 6. 2-D antenna directivity function.

temperature and the antenna directivity input data, respectively.

orbit semi-major axis	7159.493 km
orbit argument of perigree	90°
orbit eccentricity	0.001165
orbit descending node local time	10 h 5 min (a.m.)
orbit inclination	98.549°
orbit mean altitude	800 km
Earth equatorial radius	6378.137 km
Earth temperature	288 K
Earth angular aperture	1.1°
Moon temperature	200 K
Moon angular aperture	0.26°
Sun temperature	5770 K
Sun angular aperture	0.27°

Figures 7 and 8 report Sun and Moon antenna temperature plots and the corresponding scenarios

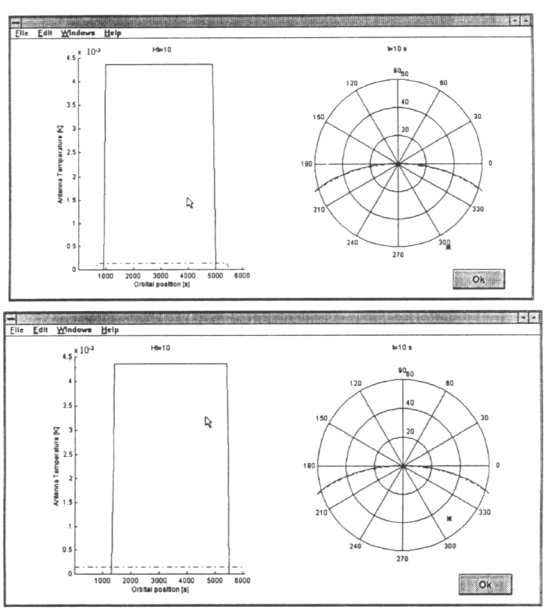

Fig. 7. Sun (solid line) and Moon (dash-dot line) antenna temperature plots for 10 km tangent height (on the left) and corresponding scenarios for $t = 10$ s orbital position (on the right) considering one orbit at autumn equinox and winter solstice, respectively.

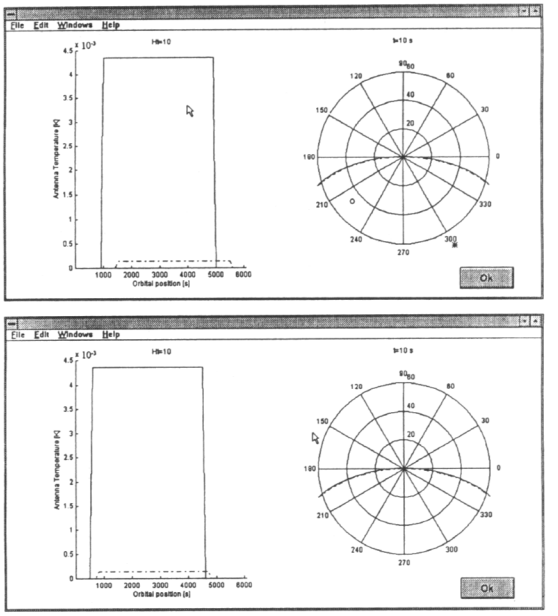

Fig. 8. Sun (solid line) and Moon (dash-dot line) antenna temperature plots for 10 km tangent height (on the left) and corresponding scenarios for $t = 10$ s orbital position (on the right) considering one orbit at spring equinox and summer solstice, respectively.

considering the four simulations. For each simulation, there are displayed, on the left, Sun (solid line) and Moon (dash-dot line) temperature profiles as functions of orbital time for a given tangent height (10 km), and, on the right, the corresponding antenna scenario for a given orbital position. At this scale, the Earth horizon dash-dot line is almost superimposed on the solid line that represents the upper limit of the atmosphere. In the same figure, the star represents the Sun and the circle represents the Moon. Figures 7 and 8 clearly show the effects on Sun and Moon apparent temperatures caused by their shadowing.

Figure 9 refers to the orbit at the autumn equinox. It displays, on the left, T_A (solid line), T_A^{At} (dashed line), and T_A^E (dot line) profiles as functions of the tangent height, for a given orbital time, while, on the right, the antenna scenario for a given tangent height

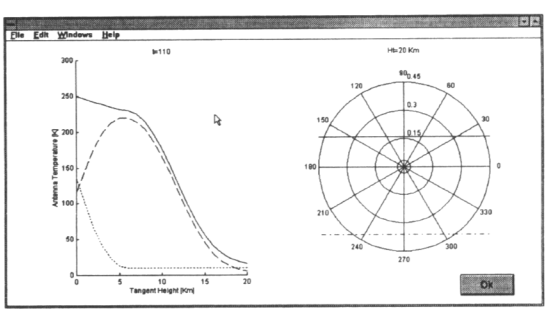

Fig. 9. Total (solid line), atmosphere (dashed line) and Earth (dot line) antenna temperature plots for a given orbital time ($t = 110$ s) (on the left) and the corresponding scenario for 20 km tangent height (on the right) considering one orbit at autumn equinox.

value is shown. The dash-dot line is the horizon of the Earth and the solid line represents the upper limit of the atmosphere. It is interesting to note that for low values of the tangent height the total antenna temperature increases because of the contribution of the Earth. In fact, in this case the Earth begins to enter the antenna Main Beam region.

Since the temperature profiles are independent of seasons, for the sake of brevity the results of the other simulations are not reported.

CONCLUSIONS

A new software tool for limb sounder measurement scenario simulation was performed by the authors within the pre-phase "A" study of MASTER (millimeter-wave acquisition for stratosphere/troposphere exchange research) mission, presently sponsored by the European Space Agency. The objective of the simulator is to generate antenna temperature maps which include contributions from Sun, Moon, Earth, atmosphere and cold space, given a user-defined antenna directivity and satellite orbit data. The software, that adopts graphic interfaces, was implemented under MATLAB as a mathematical package and was built following a modular architecture.

Several simulations, corresponding to one orbit at autumn equinox, at winter solstice, at spring equinox and at summer solstice, were performed to simulate measurement scenarios and, therefore, to evaluate the antenna temperature contributions due to the different source emissions. The output antenna temperature plots clearly show the effects and contributions of each celestial radiation source. The simulations will allow the operative parameters of MASTER limb sounder mission to be defined.

Acknowledgements—The work was performed under funding from the Earth Observation Programme of the European Space Agency.The authors really want to thank Dr. C. Rubertone and Dr. P. Spera, from Alenia Spazio S.p.A., and Prof. S. Vetrella, from University of Naples, who gave them the possibility to start and accomplish this interesting study. Special thanks is for Mr Marco Bortone, without whose precious help the MASTER software package would have never been done.

REFERENCES

1. Ulaby, F. T., Moore, R. K. and Fung, A. K., *Microwave Remote Sensing*, Vol. III. Artech House, Dedham, MA, 1986.
2. Cortesi, U., Luzi, G., Girard, R., Keskinen, K., Oricchio D. and Spera, P., Limb sounding technique for tropospheric observations: MASTER current design status. Workshop on Millimeter Wave Technology and Application, ESA WPP 098, December 1995.
3. Moccia, A., Vetrella, S. and D'Errico, M., *Twin Satellite Orbital and Doppler Parameters for Global Topographic Mapping*. EARSeL Advances in Rem. Sens., in press (1996).
4. Wertz, J. R. (ed.), *Space Attitude Determination and Control*. Reidel, Boston, 1978.
5. Ulaby, F. T., Moore, R. K. and Fung, A. K., *Microwave Remote Sensing*, Vol. I. Addison-Wesley, Reading, MA, 1981.